Carcinogenesis vol.34 no.2 pp.426–435, 2013
doi:10.1093/carcin/bgs333
Advance Access publication October 26, 2012

miR-15a and miR-16 affect the angiogenesis of multiple myeloma by targeting VEGF

Chun-Yan Sun*,†, Xiao-Mei She†, You Qin, Zhang-Bo Chu, Lei Chen, Li-Sha Ai, Lu Zhang and Yu Hu*

Institute of Hematology, Union Hospital, Tongji Medical College, Huazhong University of Science and Technology, Wuhan 430022, China

*To whom correspondence should be addressed. Tel: +86-27-85577422; Fax: +86-27-85776343;
Email: ayan0618@163.com
Correspondence may also be addressed to Chun-Yan Sun.
Email: sunchunyan66@gmail.com

Deregulated microRNAs (miRNAs) and their roles in cancer development have attracted much attention. Two miRNAs, miR-15a and miR-16, which act as putative tumor suppressor by targeting the oncogene *BCL2*, have been implicated in cell cycle, apoptosis and proliferation. In this study, we investigated the possible role of miR-15a/16 in the angiogenesis of multiple myeloma (MM). Using a stem-loop quantitative reverse transcription–PCR, we analyzed miR-15a/16 expressions in bone marrow samples from newly diagnosed MM patients and a panel of MM cell lines. miRNA transfection, western blotting analysis and assay of luciferase activity were used to examine whether vascular endothelial growth factor (VEGF) is the target of miR-15a/16. The functional roles of miR-15a/16 on tumorigenesis and angiogenesis were examined by *in vitro* angiogenesis models and *in vivo* tumor xenograft model. We showed that miR-15a and miR-16 were significantly underexpressed in primary MM cells as well as in MM cell lines. The aberrant expression of miR-15a/16 was detected especially in advanced stage MM. In human MM cell lines and normal plasma cells, expression of miR-15a/16 inversely correlated with the expression of VEGF-A. Western blotting combined with the luciferase reporter assay demonstrated that VEGF-A was a direct target of miR-15a/16. Ectopic overexpression of miR-15a/16 led to decreased pro-angiogenic activity of MM cells. Finally, infection of lentivirus-miR-15a or lentivirus-miR-16 resulted in significant inhibition of tumor growth and angiogenesis in nude mice. This study suggest that miR-15a/16 could play a role in the tumorigenesis of MM at least in part by modulation of angiogenesis through targeting VEGF-A.

Introduction

MicroRNAs (miRNAs) are a class of 22-nucleotide non-coding RNAs, which are evolutionarily conserved and function as negative regulators of gene expression. Through the specific targeting of the 3′ untranslated regions (UTRs) of multicellular eukaryotic messenger RNAs (mRNAs), miRNAs down-regulate gene expression by either inducing degradation of target mRNAs or impairing their translation (1). As a new class of regulatory molecules, miRNAs exert a broad range of biological events, including cell growth, differentiation, apoptosis, fat metabolism and viral infection (2–6). Most importantly, it has been suggested that alterations in miRNAs expression play a critical role in the pathogenesis of most of human cancers (7). Furthermore, functional studies of individual miRNAs have shown that they appear to function in a tissue-specific manner, either as tumor suppressor genes or oncogenes (8). miRNAs expression profiles have been used successfully to classify various types of tumors by developmental lineage and state of differentiation (9,10). Although a large number of miRNAs have been identified to date, the role for many of them in tumorigenesis and the underlying mechanisms are still poorly understood. One mechanism by which these miRNAs may modulate tumorigenicity is by controlling the production of angiogenic factors, and therefore neovascularization. The first evidence of involvement of miRNAs in tumor angiogenesis came from the miRNA cluster miR-17–92, which is significantly up-regulated in Myc-induced tumors and has been shown to target antiangiogenic proteins specifically. Consistently, overexpression of miR-17–92 in Ras cells enhances tumor vessel growth (11). Another miRNA that promotes angiogenesis in tumor models is miR-378, which enhances cell survival and angiogenesis by targeting suppressor of fused homolog and tumor suppressor candidate 2, both of which are tumor suppressors (12).

Multiple myeloma (MM) is an incurable B-cell neoplasm characterized by tumor cell infiltration of the bone marrow, osteolytic lesions and angiogenesis in the vicinity of the tumor cells (13). Recent evidence highlights the critical role of angiogenesis in the progression of MM (14,15). The pathophysiology of myeloma-induced angiogenesis is complex and involves either the direct production of angiogenic molecules by myeloma cells or their induction in the microenvironment (16). Among pro-angiogenic molecules that trigger the angiogenic switch during myeloma progression, vascular endothelial growth factor (VEGF) has been identified to play a key role in sustaining angiogenesis (17,18). Several studies have demonstrated that myeloma cells directly produce VEGF and induce VEGF secretion by bone marrow stromal cells (17–19). An increased serum level of VEGF has been correlated with disease progression and poor prognosis (20,21). Moreover, VEGF also exerts direct effects on MM cell proliferation, migration and drug resistance (22,23).

There are still few published data concerning miRNA that contribute to the expression of VEGF. Hua *et al.* have shown that VEGF is predicted to be targeted by multiple miRNAs, including miR-15b, miR-16, miR-20a and miR-20b. Transfection of these miRNAs into CNE cells (an human nasopharyngeal carcinoma cell line) can inhibit VEGF expression (24). More recently, Roccaro *et al.* have shown that miR-15a/16 are decreased or totally absent in relapsed/refractory MM patients, and miR-15a/16 are critical regulators of MM pathogenesis. miR-15a/16 inhibits MM cell-triggered endothelial cell growth and capillary formation *in vitro*. Transfection of pre-miR-15a and pre-miR-16 into MM cells can significantly inhibit VEGF secretion, but definitive proof of the regulation of VEGF by these miRNAs in MM remains to be demonstrated (25).

The primary aim of this study was to investigate the expression levels of miR-15a and miR-16 in MM and their correlations with disease stage. Secondly, to investigate whether VEGF-A was a target of miR-15a and miR-16 and the functional roles of miR-15a and miR-16 on angiogenesis of MM *in vitro* and *in vivo*.

Design and methods

Cells

Plasma cells were obtained from bone marrow samples from 37 newly diagnosed cases of MM, 6 patients with monoclonal gammopathy of undetermined significance (MGUS) and 18 healthy controls. All control cases were fever patients who received bone marrow biopsy but shows normal marrow cell morphology. Mononuclear cells were isolated by Ficoll-Hypaque gradient centrifugation. Plasma cells were obtained using $CD138^+$ microbead selection (Miltenyi Biotec, Auburn, CA) according to the manufacturer's instructions. Purity of plasma cells was assessed by FACscan analysis and was found to be >95%. Written informed consents were obtained from all patients and healthy controls, and these studies were approved by the institutional review board of Huazhong University of Science and Technology.

Human MM cell lines RPMI-8226, ARH-77, OPM-2, U266 and NIH929 were obtained from the American Type Culture Collection

Abbreviations: bFGF, basic fibroblast growth factor; BMEC, bone marrow-derived endothelial cell; GFP, green fluorescent protein; HGF, hepatocyte growth factor; IL-6, interleukin-6; miRNAs, microRNAs;MGUS, monoclonal gammopathy of undetermined significance; MM, multiple myeloma; mRNAs, messenger RNAs; UTRs, untranslated regions; VEGF, vascular endothelial growth factor; WT, wild-type.

†These authors contributed equally to this work.

(ATCC, Manassas, VA). The KM3 cell line was kindly provided by Dr Jian Hou (Senond Military Medical University, Shanghai, China). All the tumor cell lines were maintained in culture in RPMI-1640 medium (Hyclone, Logan, UT) supplemented with 10% fetal bovine serum (Gibco, Grand Island, NY) and antibiotics (100 units/ml penicillin and 100 μg/ml streptomycin) in an atmosphere of 5% CO_2 at 37°C. Bone marrow-derived endothelial cell (BMEC), an immortalized human bone marrow microvascular endothelial cell line by transfection with SV40, was a gift of Dr Carlton R.Cooper (University of Delaware, Newark, DE). Cultures were maintained in Dulbecco's modified Eagle's medium with high glucose, with 10% fetal bovine serum, 25 mM *N*-2-hydroxyethylpiperazine-*N*′-2-ethanesulfonic acid buffer, 100 units/ml penicillin and 100 μg/ml streptomycin.

miRNA transfection

miRNA precursors, antisense inhibitor or controls were all purchased from Ambion (Austin, TX). Transfection was performed with Lipofectamine 2000 (Invitrogen, Carlsbad, CA) following the manufacturer's protocol. Oligonucleotides were used at final concentration of 50 nM in antibiotic-free opti-modified Eagle's medium (Invitrogen). The transfection efficiency was about 90% as assessed by siGLO® Green Transfection Indicator (Dharmacon). MiRNA expressions were validated by real-time reverse transcription–PCR (RT–PCR). The conditioned media (CM) and cell extracts were prepared for analysis 48 h after the transfection.

Generation of lentiviral vectors and gene transfer

To generate lentivirus-encoding miR-15a (LV-miR-15) and miR-16 (LV-miR-16), a 307 bp fragment carrying pre-miR-15a or a 309 bp fragment carrying pre-miR-16-1 were amplified from human genomic DNA and subcloned into the lentiviral expression vector pGC-FU (GeneChem, Shanghai, China). The PCR primers used are as follows: miR-15a-5.1, 5′-*CGGCCGCGACTCTAG*ATATTC TTTAGGCGCGAATGTG and miR-15a-3.1,5′-*ATAAGCTTGATATCG* AGAGTATGGTCAACCTTAC, miR-16-1-5.1 ATCG*GAATTC*TGAA AAGGTGCAGGCCATAT and miR-16-1-3.1 ATCG*GAATTC* TAAAAATAACAAGATTATCAATAATACTG. The constructs were confirmed by DNA sequencing, and then co-transfected with pHelper 1.0 and pHelper 2.0 Packing Plasmid (GeneChem) into 293T packing cells using Lipofectamine 2000 (Invitrogen). Forty-eight hours after transfection, the supernatant was collected, centrifuged at 1000 r.p.m. for 5 min and filtered through 0.22 μm pore nitrocellulose filters. LV-GFP, a control virus, was similarly produced. The virus titer was quantified according to the expression level of green fluorescent protein (GFP) following the manufacturer's instruction.

MM cells were transfected with LV-miR-15a/16 or LV-GFP in the presence of 4 μg/ml polybrene (Sigma–Aldrich, St Louis, MO) at a multiplicity of infection of 10 and centrifuged at 1800 r.p.m. for 45 min. Thereafter, cells were cultured for 48 h and analyzed by fluorescence-activated cell sorting (BD Biosciences, Bedford, MA). Expression of mature miR-15a or miR-16 was confirmed by real-time RT–PCR.

Assay of luciferase activity

3′-UTR of VEGF-A predicated to interact with miR-15a and miR-16 were amplified from human genomic DNA and cloned downstream of the stop codon in PGL3-control vector (Promega, Madison, WI). The construct was designated as wild-type (WT) 3′UTR. The mutated 3′UTR were amplified by PCR with WT 3′UTR as the template using the site-directed mutagenesis kit (Takara, Dalian, China), inserted into the same reporter vector and named mutant A, mutant B and mutant C, respectively. The sequences of primers used for luciferase reporter plasmids construction were shown in Table I. pRL-TK vector was used as an internal control reporter. Cells were harvested 48 h after co-transfection of miRNA with reporter vector and assayed with Dual Luciferase Assay (Promega) according to the manufacturer's protocol.

Western blotting analysis

Protein extraction and western blotting were performed as described in detail previously (26). Briefly, 30–60 μg cell lysates were subjected to sodium dodecyl sulfate–polyacrylamide gel electrophoresis, transferred to nitrocellulose membranes and then blotted with an anti-VEGF antibody (1:1000) (sc-152; Santa Cruz Biotechnology, Santa Cruz, CA), followed by horseradish peroxidase-conjugated secondary antibody (Transduction Laboratories, Lexington, UK), and visualized by Enhanced Chemiluminescence (Amersham Biosciences, Piscataway, NJ). The membrane was stripped using a western blot stripping buffer (Pierce, Rockford, IL) and reincubated with anti-β-actin antibody (1:2000) (sc-69879; Santa Cruz Biotechnology) to control for protein loading.

Semi-quantitative RT–PCR

RNA extraction and semi-quantitative RT–PCR were performed as described in detail previously (26).

Real-time quantification of mature miR-15a and miR-16 by stem-loop RT–PCR

The total RNAs from cells were isolated using TRIzol reagent according to the manufacturer's instructions. Complementary DNA was synthesized from total RNA (1 μg) in 20 μl reactions, using reverse transcriptase (Epicentre, Madison, WI) and the RT primer for miR-15a and miR-16 or U6 obtained from Invitrogen. The reverse transcriptase reaction was performed by incubating the samples at 16°C for 30 min, 42°C for 42 min and 85°C for 5 min. For a quantitative analysis of mature miR-15a and miR-16, a stem-loop quantitative RT–PCR analysis was performed, using primers designed based on miRNA sequences released by the Sanger Institute.

The PCR reaction (25 μl) contained 1 μl of reverse transcriptase product, 2.5 μl of deoxynucleoside triphosphate (HyTest Ltd, Turku, Finland), 2.5 μl of 10× PCR reaction buffer (containing $MgCl_2$) (Promega), 1 units *of Taq* polymerase (Promega), 0.25× SYBR® Green I nucleic acid gel stain (Invitrogen) and 1 μl of the forward primer and universal reverse primer for the miRNA of interest. The PCR mixtures were incubated at 95°C for 5 min, and this was followed by 40 cycles of 95°C for 10 s, 60°C for 20 s, 72°C for 20 s and 78°C for 20 s. All PCR reactions were performed in triplicate using a Rotor-Gene 3000 real-time PCR system (Corbett Research, Mortlake, NSW, Australia). The expression of miR-15a and miR-16 were based on the $2^{-\triangle\triangle CT}$ method, using U6 as an internal control.

Collection of CM

MM cells from either miRNA precursors or control were seed on six-well plates at 2×10^6/ml in RPMI-1640 supplemented with 2% fetal bovine serum. After culture for 24 h, the supernatant was collected and centrifuged at 1200 r.p.m. and 12 000 r.p.m. for 10 min to remove cell debris.

Enzyme-linked immunosorbent assay

Detection of VEGF as well as three other well-known angiogenic cytokine, basic fibroblast growth factor (bFGF), hepatocyte growth factor (HGF), and interleukin-6 (IL-6), in culture supernatants were achieved by enzyme-linked immunosorbent assay (R&D System, Minneapolis, MN) according to the manufacturer's instructions.

In vitro angiogenesis assays

BMEC cells were plated at a density of 5×10^3 cells/well in a 96-well plate in triplicate. CM from transfected MM cells was added at a dilution of 1:1 into BMEC cell cultures. After 48 h of incubation at 37°C, relative cell growth rate was measured using an 3-(4,5-dimethylthiazole-2-yl)-2,5-diphenyl tetrazolium bromide based assay as described previously (27). The chemotactic motility and morphological differentiation of BMEC were also performed according to the methods described previously (27).

Table I. Primers used for PCR

Primer name	Sequence
WT 3′UTR forward	5′- CCG ctc gag GCC GGG CAG GAG GAA GGA G-3′
WT 3′UTR reverse	5′-ATA AGA ATg cgg ccg cTG AGA TCA GAA TTA AAT TCT TTA ATA C-3′
Mutant A forward	5′-GGATTCGCCATTTTATTTTTCTATCGATCAAATCACCGAGCCCGGAAGAT-3′
Mutant A reverse	5′-ATCTTCCGGGCTCGGTGATTTGATCGATAGAAAAATAAAATGGCGAATCC-3′
Mutant B forward	5′-GGAGCTTCAGGACATTGCACACGATTGGGGATTCCCTCCACATG-3′
Mutant B reverse	5′-CATGTGGAGGGAATCCCCAATCGTGTGCAATGTCCTGAAGCTCC-3′

For rescue experiments, pcDNA-VEGF-A was constructed to exogenously express VEGF-A by introducing a BamHI–EcoRI fragment containing the VEGF-A mRNA without its 3′-UTR sequence into the same sites in pcDNA3.1 (Invitrogen). VEGF-A was ectopically expressed in RPMI-8226 cells transfected with miR-15a or control miRNA, and CM was collected for *in vitro* angiogenesis assays and MM cells were used for western blot analysis.

In vivo tumor xenograft model

Female BALB/C nude mice aged 6–8 weeks were purchased from Beijing Hua Fukang Bioscience Company (Beijing, China) and were housed and monitored in a pathogen-free environment. RPMI-8226/LV-GFP and RPMI-8226/LV-miR-15a cells were harvested, washed with phosphate-buffered saline and resuspended in phosphate-buffered saline containing 50% matrigel (BD Biosciences) at a concentration of 2×10^8/ml. Mice were divided into two groups, one for RPMI-8226/LV-GFP and the other for RPMI-8226/LV-miR-15a. A mixture of 2×10^7 cells were injected subcutaneously into the left collar of nude mice. Serial measurements of xenograft growth were performed, and tumor volume was calculated using the formula $V = 4\pi/24 \times a \times b^2$, where a and b represents the larger and smaller tumor diameters, respectively. The tumors were removed and sectioned for immunohistochemistry staining of anti-CD31 (BD PharMingen, San Jose, CA) to assess microvessel density as described previously (28). All animal studies were approved by the Committee on Animals Handling of Huazhong University of Science and Technology.

Six-week-old male NOD/SCID mice (Beijing Hua Fukang Bioscience Company, Beijing, China) were intravenously injected with 2×10^6 GFP-labeled RPMI-8226 cells after 200 rads gamma irradiation and were bred and maintained in the animal resources facility of Tongji Medical College. About 20 μg synthetic miR-15a, miR-16 or negative control miRNA (miR-NC) (Dharmacon Research, Lafayette, CO) was formulated with MaxSuppressor *in vivo* RNALancerII, a lipid-based delivery reagent (BIOO Scientific, Austin, TX), according to manufacturer's instructions. Formulated miRNA was administered intravenously by tail vein injections on the days 1, 4, 9, 12, 17 and 20 for a total of six injections at a concentration of 1 mg/kg each time. Mice were observed daily, and five animals per group were killed at 6 weeks following paralysis. Images were investigated with Luminescent Image Analyzer LAS-4000 (Fujifilm, Stamford, CT). The 10 remaining mice per group were monitored for signs of disease and overall survival.

Statistical analysis

All data are expressed as the mean ± SD. One-way analysis of variance, with the Mann–Whitney *U*-test as non-parametric alternatives, was used for the analysis of differences between groups. Results were considered significantly different for P values <0.05. The significance of differences in overall survival was analyzed by Kaplan–Meier curves and log-rank test. All experiments were performed at least three times to insure reproducibility of the results.

Results

miR-15a and miR-16 are down-regulated in MM cells and specific down-regulation of miR-15a and miR-16 correlate with advanced stage

Recently, miR-15a/16 were found to be down-regulated in some hematological tumors and were considered to regulate cancer-related genes related with apoptosis, cell cycle, cell proliferation and survival (26,29,30). However, the functional contributes of miR-15a/16 associated with tumor angiogenesis have not been experimentally established. To evaluate the possible effects of miR-15a/16 on the angiogenesis of MM, we first verified their expression in MM cells. As shown in Figure 1A and 1B, real-time PCR data revealed that miR-15a and miR-16 were down-regulated in 4 of 14 stage I and II and 21 of 23 stage III MM cells studied (ISS stage). The expression of miR-15a and miR-16 were remarkably lower in stage III MM patients (n = 23), whereas it were significantly higher in healthy individuals (n = 18) and stage I and II MM patients (n = 14). MGUS is generally believed to represent a pre-malignant form of MM, so we also examined expression of miR-15a and miR-16 in this condition (n = 6). We confirmed that miR-15a and miR-16 were significantly down-regulated only in advanced stage of MM patients but not in MGUS or early stage MM patients. No significant difference was found between stage I and II MM patients, MGUS and healthy individuals. Because MM patients with advanced stage disease have increased bone marrow angiogenesis (31), we speculate that alterations of miR-15a and miR-16 could be involved in angiogenesis of MM.

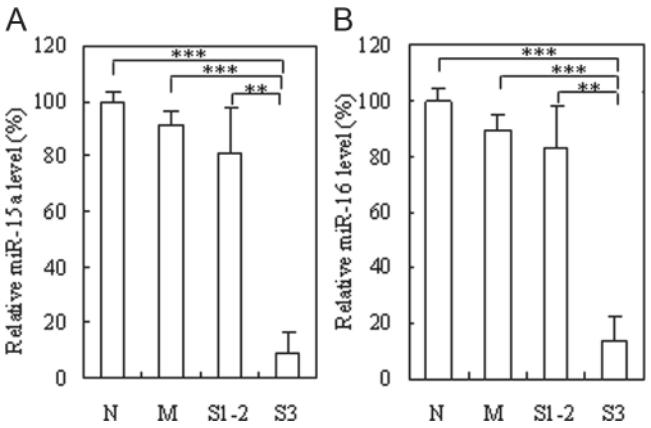

Fig. 1. Expression of miR-15a and miR-16 were down-regulated in advanced stage MM specimens. miR-15a (**A**) and miR-16 (**B**) expression in MM patient, MGUS or healthy donor bone marrow CD138+ cells were determined by quantitative RT–PCR method. Results were normalized against the expression level of U6 small nuclear RNA in each sample. The differences of miR-15a and miR-16 expression levels between disease stages were analyzed by Wilcoxon rank sum test. S1-2: stage I, II MM (n = 14), S3: stage III MM (n = 23), M: MGUS (n = 6), N: an average of expression level of all 18 healthy donor bone marrow CD138+ cells (n = 18). $^{**}P < 0.01$, $^{***}P < 0.001$.

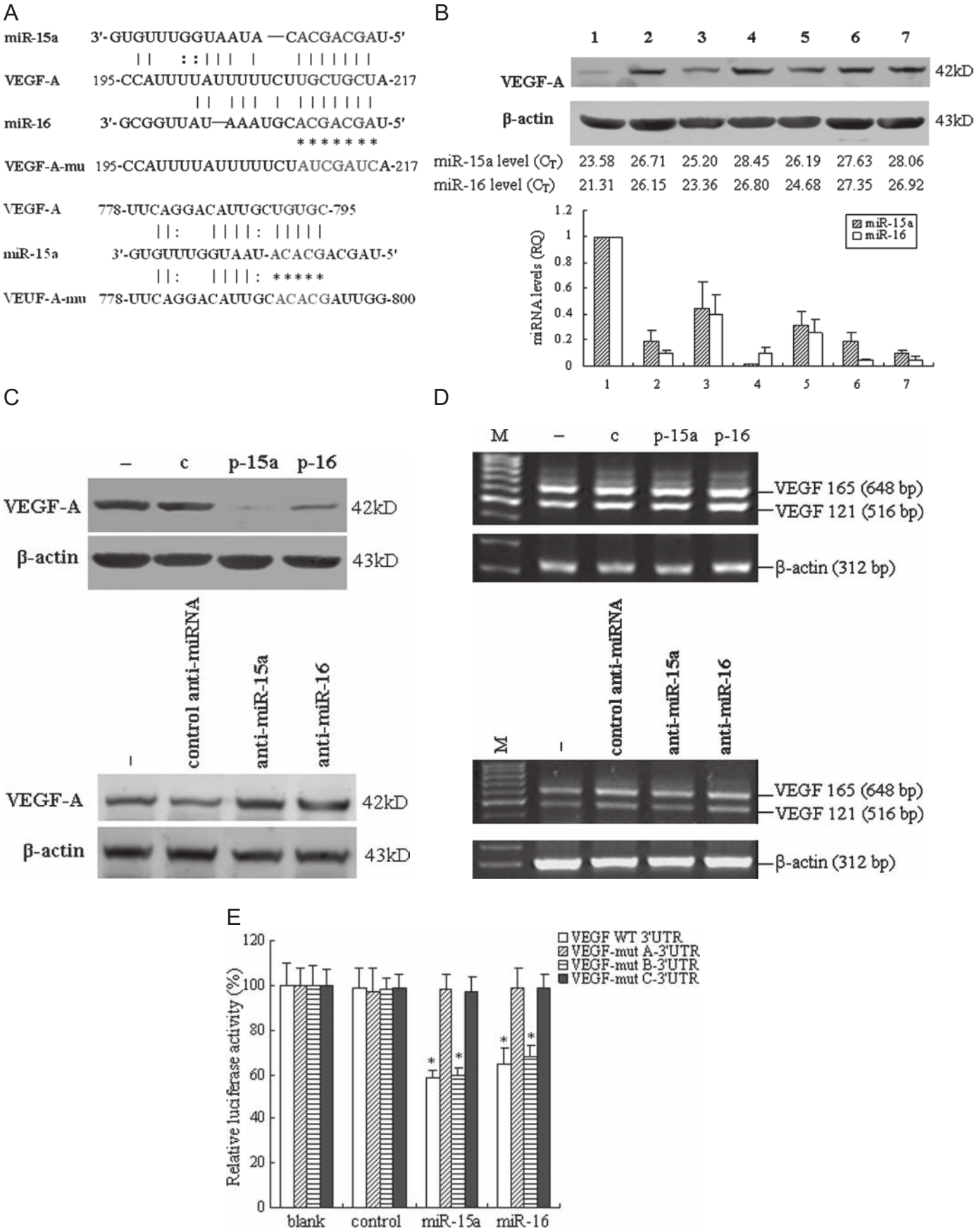

Fig. 2. Targeting of VEGF-A by miR-15a and miR-16. (**A**) Sequence alignment of human miR-15a and miR-16 with 3′-UTR of VEGF-A. The seed sequence of miR-15a and miR-16 matches 3′-UTR of VEGF-A (upper). Mutation of the 3′UTR of VEGF-A for creating the mutant luciferase reporter construct (lower).

VEGF-A is a target of post-transcriptional repression by miR-15a and miR-16

We next searched for miR-15a/16 putative targets in MM as predicted by commonly cited programs such as TargetScan (32), microRNA.org (33) and TargetRank (34). VEGF-A was found to be among the predicted high confidence targets by all three methods. 3′-UTR of human VEGF-A harbors two putative region that matches to the seed sequence of has-miR-15a and has-miR-16 (Figure 2A). To experimentally validate the possible relationship inversely linking VEGF-A and miR-15a/16, we first verified their expression in human MM cell lines. A number of human MM cell lines were analyzed for VEGF-A expression by western blotting, and miR-15a/16 levels were analyzed by RT–PCR. In these MM cell lines, U266, NIH929 and OPM-2 were established from relapsed or refractory MM patients, RPMI-8226 cell line was established from IgG-λ type MM patient and ARH-77 has now been considered as an EBV-transformed B lymphoblastoid cell line. As shown in Figure 2B, significantly decreased expression of miR-15a and miR-16 was observed in RPMI-8226, ARH-77, OPM-2 and KM3 cell lines. The miR-15a and miR-16 expression in U266 and NIH929 were mild down-regulated. High levels of VEGF-A expression were correlated with low levels of miR-15a and miR-16 expression. In order to determine whether the secretion of VEGF and other pro-angiogenic factor (bFGF, HGF, IL-6) were altered by pre-miR-15a and pre-miR-16 transfection, an enzyme-linked immunosorbent assay test was then performed. As shown in Table II, VEGF levels in pre-miR-15a and pre-miR-16-transfected cell culture supernatant were significantly decreased compared with those of non-transfected cells or transfected with miRNA precursor control. However, the secretion of bFGF, HGF and IL-6 demonstrated no significant changes between different groups. These data indicate an inverse correlation between the expression levels of miR-15a and miR-16 and the VEGF-A protein levels.

Several other miR-15/107 group members, such as miR-15b, miR-103, miR-107 and miR-195, show the same seed sequence with miR-15a and miR-16 and also many common targets (35). So, we next examined their expression in MM cells. Real-time PCR data revealed that expression of miR-103, miR-15b and miR-195 has no significant difference between normal plasma cell and various human MM cell lines, and the miR-107 expression in RPMI-8226 and OPM-2 were mild down-regulated (Supplementary Figure S1, available at *Carcinogenesis* Online). However, the levels of VEGF-A expression were uncorrelated with levels of miR-107 expression.

To examine whether VEGF-A is indeed the target of miR-15a and miR-16, we transiently transfected miR-15a and miR-16 into RPMI-8226 cells to evaluate target gene expression. Western blotting revealed that the VEGF-A protein was clearly reduced in pre-miR-15a- (81%) and pre-miR-16- (57%) transfected cells, as compared with cells transfected with the control pre-miRNA (Figure 2C, upper). In contrast, knockdown of miR-15a and miR-16 by antisense oligonucleotides complementary to either miR-15a or miR-16 in U266 cells, which express relative high levels of endogenous miR-15a and miR-16, increased the protein level of VEGF-A (Figure 2C, lower). The results indicated that VEGF-A is an actual target of miR-15a and miR-16 in MM cells.

To investigate whether miR-15a/16 targeted VEGF-A mRNA for degradation, a semi-quantitative RT–PCR evaluation was carried out on RNA isolated from control and transfected cells. The data showed comparable steady-state mRNA levels of VEGF-A (Figure 2D), providing evidence that miR-15a and miR-16 repressed VEGF-A expression at the translational level.

To verify the putative direct interaction between miR-15a/16 and the VEGF 3′-UTR, the 3′-UTR segments of VEGF predicted to interact with miR-15a and miR-16 were cloned into the firefly luciferase report plasmid construction. The putative target sites for the miR-15a and miR-16 seed sequence were predicted to be located within the VEGF 3′UTR at nucleotides 195–217 (named target site A) by TargetScan (32) and microRNA.org (33). Hua *et al.* also reported a second binding site for the miR-15a and miR-16 seed sequence at nucleotides 703–944 (named target site B (24)). To identify which fragments of the VEGF 3′-UTR interact with miR-15a and miR-16, three mutated PGL3-VEGF-mut-3′-UTR were constructed. Mutant A contains the inactivated target site A in nucleotides 195–217, mutant B contains the inactivated target site B in nucleotides 703–944 of the VEGF 3′-UTR, whereas mutant C bears both A and B inactivated target sites. Luciferase assays showed that compared with control miRNA, miR-15a and miR-16 significantly decreased the luciferase activity of reporter plasmid with the intact VEGF 3′UTR. However, miR-15a and miR-16 had no effect on luciferase activity of PGL3-VEGF-mut A-3′-UTR and PGL3-VEGF-mut C-3′-UTR, but miR-15a and miR-16 still significantly reduced the luciferase activity of PGL3-VEGF-mut B-3′-UTR. As shown in Figure 2E, if site B was mutated, the luciferase activity was dramatically decreased by miR-15a and miR-16. However, once site A or both target sites were mutated, the luciferase activity of reporter plasmid was no longer affected by miR-15a and miR-16 at all (Figure 2E). Taken together, these data indicate

Table II. Concentration of angiogenic factors in CM from control and transfected RPMI-8226 cells

CM of RPMI-8226 cells	VEGF (pg/10^6 cells/ml) (mean ± SD)	bFGF (pg/10^6 cells/ml) (mean ± SD)	HGF (pg/10^6 cells/ml) (mean ± SD)	IL-6 (pg/10^6 cells/ml) (mean ± SD)
Non-transfected cells	865 ± 126	12.6 ± 3.1	1028 ± 210	Undetectable
miRNA precursor control	890 ± 152	11.8 ± 2.8	985 ± 167	Undetectable
Pre-miR-15a	201 ± 48	12.8 ± 2.5	1052 ± 145	Undetectable
Pre-miR-16	158 ± 32	11.2 ± 2.7	961 ± 208	Undetectable

←
(**B**) miR-15a, miR-16 and VEGF-A expression in MM cell lines. RNA and protein samples, prepared from various human MM cell lines, were subjected to analyses of miR-15a and miR-16 expression by quantitative RT–PCR, and VEGF levels were analyzed by western blotting (upper). Relative expression level of miR-15a and miR-16 in MM cell lines compared with normal plasma cell (lower). Results were normalized against the expression level of U6 small nuclear RNA in each sample. Lane 1, normal plasma cell; lane 2, RPMI-8226; lane 3, U266; lane 4, ARH-77; lane 5, NIH 929; lane 6, OPM-2; lane 7: KM3. RQ, relative quantification. (**C**) Western blotting analysis of VEGF-A. miR-15a and miR-16 reduces VEGF-A protein expression (upper). Non-transfected RPMI-8226 cells (–) and RPMI-8226 cells transfected with pre-miR-15a (p-15a), pre-miR-16 (p-16) or miRNA precursor control (c) were harvested and subjected to western blotting for VEGF-A expression. Analysis of β-actin was performed as a loading control. Knockdown of miR-15a and miR-16 inducing VEGF-A expression (lower). U266 cells were transfected with anti-miR-15a, anti-miR-16 inhibitor or anti-miRNA inhibitor control. Non-transfected U266 cells were used as control. Whole cell lysates were subjected to western blotting using anti-VEGF and anti-β-actin antibodies. (**D**) RT–PCR evaluation of VEGF-A mRNA. RNA prepared from the same RPMI-8226 cells (upper) and U266 cells (lower) utilized in C was subjected to RT–PCR of VEGF-A. β-actin was used for control. (**E**) Dual luciferase assay was performed in RPMI-8226 cells transfected with luciferase construct alone (blank) or co-transfected with pre-miR-15a or pre-miR-16-1 or control precursor miRNA. Firefly luciferase construct containing either WT (3′UTR) or mutant target site of VEGF 3′UTR (mutant A, mutant B and mutant C) was generated and transfected as indicated. Firefly luciferase activity was normalized to Renilla luciferase activity. Error bars represent standard deviation and were obtained from three independent experiments.*$P < 0.05$.

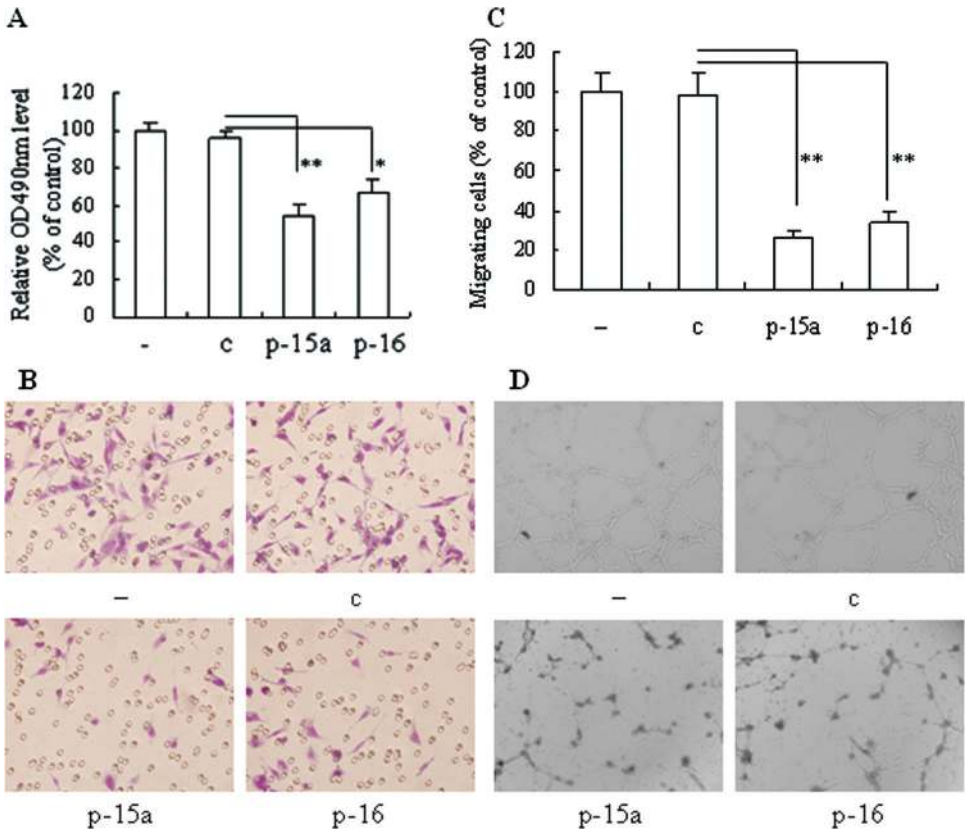

Fig. 3. miR-15a and miR-16 exert antiangiogenic activity *in vitro*. (**A**) RPMI-8226 cells in logarithm growing period were transfected with either pre-miR-15a (p-15a), pre-miR-16 (p-16) or miRNA precursor control (c). Non-transfected RPMI-8226 cells were used as control (–). CM obtained from RPMI-8226 cells was added at a dilution of 1:1 into BMEC cell cultures. After incubation for 48 h, the proliferation of BMEC cells was detected by 3-(4,5-dimethylthiazole-2-yl)-2,5-diphenyl tetrazolium bromide assay. Transfection with miR-15a and miR-16 in RPMI-8226 cells inhibited cell growth of BMEC cells. Data represent the mean ± SD ($n = 4$). *$P < 0.05$, **$P < 0.01$. (**B**) Cell migration was evaluated using a 24-transwell chamber with 8 µm pore insert. The migration ability of BMEC cells were significantly affected by miR-15a and miR-16 overexpression in RPMI-8226 cells (Wright's stain, Olympus DP70, magnification ×200). (**C**) Quantification of the migration capability of BMEC cells. (**D**) Overexpression of miR-15a and miR-16 also impaired morphological differentiation of BMEC cells (Olympus DP70, magnification ×100), as evaluated by the tube formation assay.

that VEGF 3′UTR is a specific direct target of miR-15a/16, and miR-15a/16 has targeting activities only at nucleotides 195–217 of the VEGF 3′-UTR. In this study, the target site B (nucleotides 703–944) is not a functional miR-15a/16 binding site. We speculated that it is probably because different cell lines were involved in this study, and the same miRNA may target different genes in different cells.

Expression of miR-15a and miR-16 suppresses pro-angiogenic activity of MM cells

VEGF is known to play a pivotal role as a regulator of pathologic angiogenesis in bone marrow microenvironment in MM. We next tested if the pro-angiogenic potential of stably transfected MM cells expressing miR-15a/16 was modified, as a consequence of the demonstrated VEGF-A reduction.

MM cells were transfected with either pre-miR-15a, pre-miR-16 or miRNA precursor control. 3-(4,5-Dimethylthiazole-2-yl)-2,5-diphenyl tetrazolium bromide assay was employed to measure BMEC cells proliferation. The results shown in Figure 3A suggested that proliferation of BMEC cells was inhibited in the presence of CM obtained from pre-miR-15a- and pre-miR-16-transfected RPMI-8226 cells. Regarding cell migration, CM of pre-miR-15a- and pre-miR-16-transfected RPMI-8226 cells decreased the chemotactic motility of BMEC cells by up to 46% ($P < 0.05$) as compared with CM of control precursor-transfected RPMI-8226 cells (Figure 3B and C). We next observed that the morphological differentiation of BMEC cells was also affected by miR-15a and miR-16 overexpression in RPMI-8226 cells. The reticulate capillary formation experiments in the two-dimensional matrigel showed that BMEC cells formed incomplete and fluffy tubular structures in the presence of CM obtained from pre-miR-15a- and pre-miR-16-transfected RPMI-8226 cells. In contrast, the treatment with CM obtained from control led to the formation of elongated and robust tubular structure (Figure 3D). All these results indicated that overexpression of miR-15a and miR-16 in MM cells could inhibit pro-angiogenic activity of MM cells *in vitro*.

The effect of miR-15a and miR-16 on the angiogenesis is mainly through targeting VEGF expression

As VEGF-A expression is validated to be post-transcriptionally regulated by miR-15a/16, we further sought to prove the VEGF-A dependence of the antiangiogenic activity of miR-15a/16. Because miR-15a/16 down-regulates VEGF-A through binding to 3′-UTR of VEGF-A mRNA, ectopic expression of VEGF-A by transfection of the complementary DNA that only contains the coding region of VEGF-A should escape the regulation by miR-15a/16. When one of the miRNAs, miR-15a, was transfected into VEGF-transfected RPMI-8226 cells, western blotting analysis confirmed that transfection of VEGF-A complementary DNA lacking 3′-UTR overrided VEGF-A reduction induced by miR-15a (Figure 4A). We also observed that chemotactic motility (Figure 4B and C) and reticulate capillary formation (Figure 4D) of BMEC cells suppressed by miR-15a expression was significantly increased by CM of VEGF-A stably transfected RPMI-8226 cells. These results further demonstrate

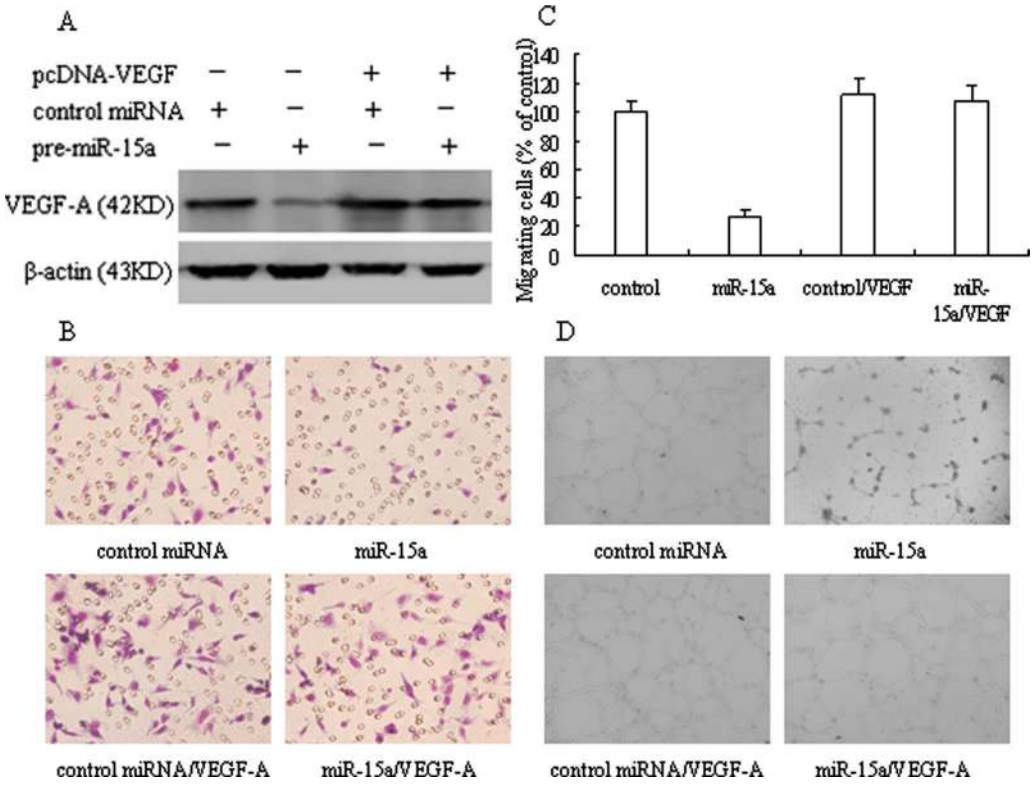

Fig. 4. The effect of miR-15a and miR-16 on the angiogenesis is mainly through targeting VEGF. (**A**) RPMI-8226 cells were stably transfected with indicated plasmids and assayed for expression of VEGF-A. CM obtained from RPMI-8226 cells in A were added at a dilution of 1:1 into BMEC cell cultures, cell migration (**B, C**) and morphological differentiation (**D**) were examined as described in Figure 3B and 3D.

that VEGF-A is a major target of miR-15a/16 and the antiangiogenic effect of miR-15a is mainly through inhibition of VEGF-A expression.

Expression of miR-15a and miR-16 suppresses tumorigenesis and angiogenesis

To explore the *in vivo* relevance of our observations, RPMI-8226 cells were infected with LV-miR-15a or LV-GFP and implanted by the subcutaneous route into the nude mice. We found that after 2 weeks of cell inoculation, 75% of mice injected with GFP-transfected MM cells developed measurable tumors. In contrast, mice injected with the miR-15a-transfected cells showed significant inhibition of tumor growth compared with controls (Figure 5A). The average tumor volume after 4 weeks for GFP-transfected cells was 672.5 mm^3, whereas the average tumor volume for miR-15a-transfected cells was 189.6 mm^3 (Figure 5B). The tumor growth reduction may be speculated to be the results of angiogenesis inhibition. To confirm this speculation, the tumors were removed and sectioned for neoangiogenesis analysis by staining with anti-CD31 antibody (Figure 5C). Quantitative analysis showed that there was significant reductions in the blood vessels present in the miR-15a group compared with control (Figure 5D). Similar results were obtained in the miR-16 group (Supplementary Figure S2, available at *Carcinogenesis* Online). Taken together, these data indicate that expression of miR-15a/16 greatly inhibited the process of tumor formation and miR-15a/16 would seem to regulate tumorigenesis via angiogenesis inhibition.

To explore the therapeutic effects of systemic delivery of miR-15a mimics *in vivo*, we used the NOD/SCID mouse model. About 2×10^6 GFP-labeled RPMI-8226 cells were injected intravenously into NOD/SCID mice after sub-lethal irradiation, then synthetic miR-15a/16 or negative control (miR-NC) miRNAs conjugated with neutral lipid emulsion were introduced via tail vein injections on the days 1, 4, 9, 12, 17 and 20 for a total of six injections. As shown in Figure 6A, the tumor burdens in mice treated with miR-NC were remarkably higher than that with miR-15a or miR-16 in 6 weeks after tail vein injection. In mice treated with miR-NC, fluorescence activity was marked visible in the skull and pelvis. In contrast, mice treated with the miR-15a or miR-16 showed significant decreased fluorescence activity. Kaplan–Meier curves and log-rank analysis showed significant prolonged overall survival of mice in miR-15a or miR-16 group compared with miR-NC group ($P < 0.05$) (Figure 6B). These results demonstrate that systemic delivery of miR-15a or miR-16 mimics can effectively cause inhibition of myeloma growth *in vivo*.

Discussion

Growing evidence has indicated that as regulation factors of gene expression, miRNAs are frequently dysregulated in a number of human malignancies, and dysregulation of miRNA is involved in tumor initiation and progression (36,37). miR-15a and miR-16 are the first two miRNAs that demonstrated the involvement of miRNAs in human cancer. Calin *et al.* found that miR-15a and miR-16 were frequently down-regulated in chronic lymphocytic leukemia and were proven to be potential tumor suppressors by targeting the oncogene *BCL2* (30,38). In this study, we found that miR-15a and miR-16 were down-regulated in about 70% of the tumor samples with respect to their normal counterparts and that down-regulation of these two miRNAs seem to be associated with advanced stage MM. These findings suggest that down-regulation of miR-15a and miR-16 could contribute to MM progression rather than initiation. This observation was consistent with a recent study reporting that miR-15a and miR-16 were down-regulated in relapsed/refractory MM compared with healthy controls (25).

Recently, accumulating evidence indicates that miRNAs have been implicated in the regulation of various aspects of angiogenesis (39–41). Although several miRNAs have been implicated in survival and

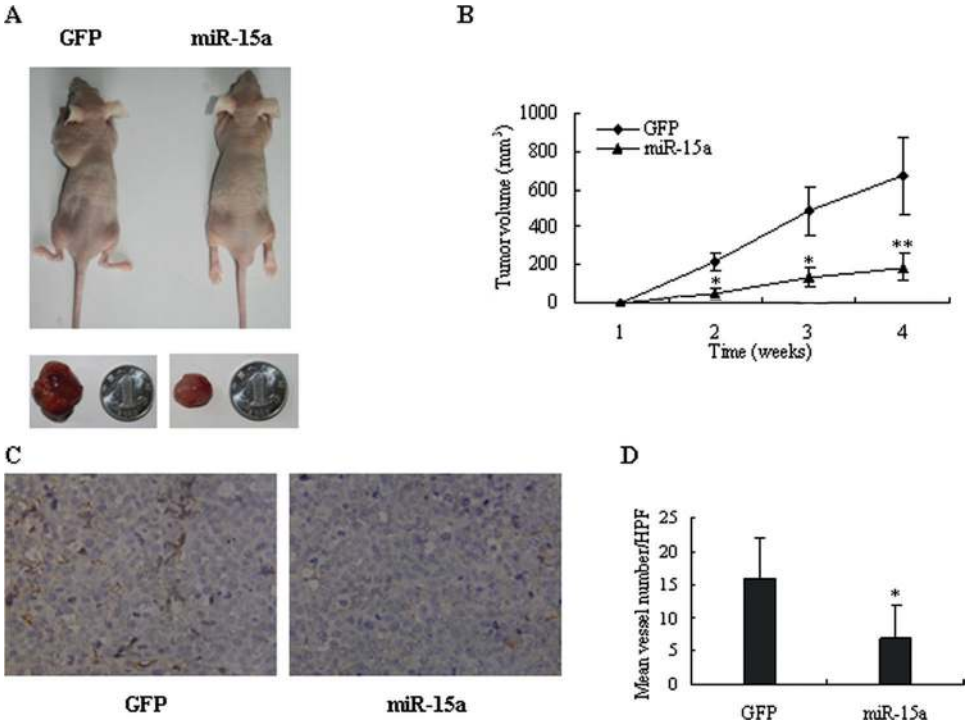

Fig. 5. Inhibitory effect of miR-15a on the tumor formation and angiogenesis *in vivo*. (**A**) RPMI-8226 cells transfected with LV-miR-15a or LV-GFP were injected subcutaneously into nude mice. Four weeks after the injection, mice were photographed and killed. (**B**) Tumor sizes were measured, and tumor growth curves were obtained. Data are presented as tumor volume in the mean ± SD ($n = 8$). *$P < 0.05$, **$P < 0.01$. (**C**) Tumors formed by cells transfected with the miR-15a or control vector were subjected to immunohistochemistry staining using anti-CD31 antibody (Olympus DP70, magnification ×400). (**D**) Bar chart shows comparisons of the mean CD31-positive vessel number per high-power field of the various tumor sections. Data are presented as mean ± SD ($n = 8$). *$P < 0.05$.

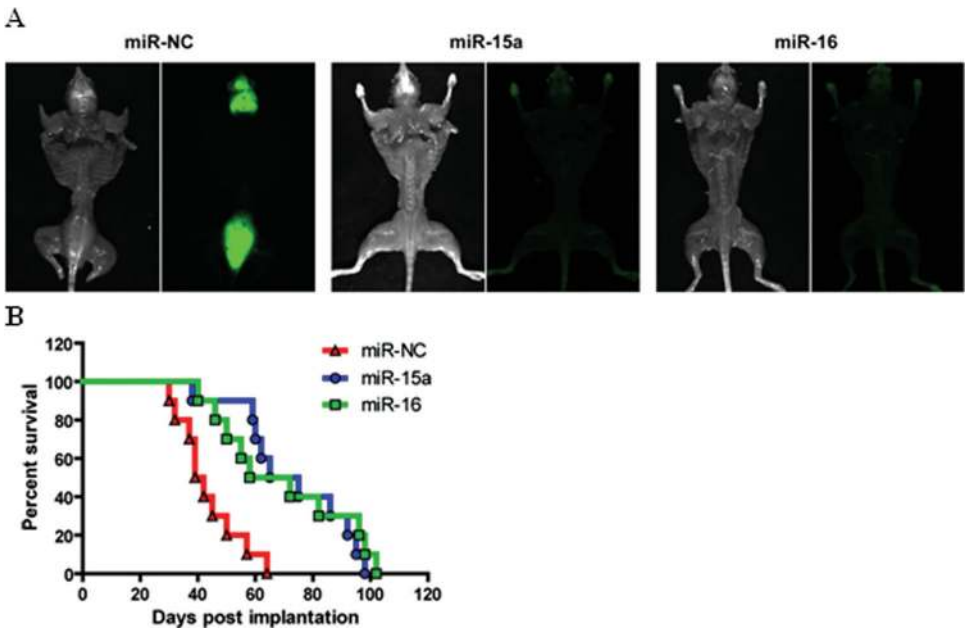

Fig. 6. Systemic delivery of miR-15a or miR-16 mimic reduces tumor burden in a NOD/SCID myeloma model. (**A**) Luminescent images of mice were taken at 6 weeks after intravenous injection of GFP-labeled RPMI-8226 cells following miR-15a/16 or negative control (miR-NC) formulated with neutral lipid emulsion. (**B**) The effects of miR-15a and miR-16 on overall survival were analyzed by Kaplan–Meier curve and log-rank test ($n = 10$).

proliferation of myeloma cells and myeloma tumor growth, there are few published data concerning the role of miRNA in the angiogenesis of MM (42,43). Our present work revealed that miR-15a and miR-16 were complementary to the VEGF-A 3′-UTR, and the interaction can inhibit the overexpression of VEGF in MM cells. Ectopic expression of miR-15a and miR-16 were able to efficiently reduce the expression of VEGF in RPMI-8226 cells and inhibit the pro-angiogenic effects of RPMI-8226. *In vivo* restoration of miR-15a and miR-16 significantly suppressed tumorigenicity of RPMI-8226 cells in nude mice and inhibited angiogenesis of tumor xenograft. These evidences

suggest that miR-15a and miR-16 are potential tumor suppressor genes in MM development, directly targeting the pro-angiogenic factor VEGF-A. Recent studies have shown that VEGF has a particular important role in the biology of MM (18). Although some anti-VEGF monoclonal antibodies and oral VEGFR inhibitors have been under clinical development for the treatment of MM, the clinical evidences revealed that some anti-VEGF agents have associated toxicity due to its disruption of normal vasculature (44). To date, re-expression of miRNAs had been suggested to hold considerable potential in tumor gene therapy (45). Thus, the restoration of miR-15a and miR-16 expression may have considerable therapeutic significance for MM. To date, few tumor suppressor miRNAs have been discovered for which the proof of concept of miRNA replacement therapy has been shown in preclinical animal models of cancer. Among these are the tumor suppressors *let-7*, miR-16, miR-34 and miR-26a (46–48). Our data provide strong evidence that systemic delivery of miR-15a and miR-16 *via* neutral lipid emulsion is a safe and effective therapeutic approach for the treatment of MM.

miR-15a and miR-16 are also frequently down-regulated in chronic lymphocytic leukemia, prostate cancer and non-small cell lung cancer (39,49,50). However, both miRNAs are frequently up-regulated in cervical cancer (51). Hence, deregulation of miR-15a and miR-16 may be different in different type of cancers, and miR-15a and miR-16 may play a dual role in tumorigenicity. In fact, such a dual nature of miRNAs in carcinogenesis and progression has been previously reported in miR-155, miR-195, miR-205 and miR-17–92 cluster (52–54). The underlying mechanisms mediating miRNAs deregulation in cancer development are still elusive. miR-15a and miR-16 are transcribed as a cluster that resides in the 13q14 chromosomal region. Although deletion of 13q14 occur in 50% MM, Corthals *et al.* demonstrated that the expression patterns of miR-15a and miR-16 in MM patients are independent of the chromosome 13 status (55). As deregulated epigenetic status in cancer often mediates the deregulation of tumor suppressors or oncogenes, we will further determine whether the deregulation of miR-15a and miR-16 is mediated by epigenetic alterations.

In summary, the findings we reported in this study presented the evidence that down-regulation of miR-15a and miR-16 associate with MM progression. miR-15a and miR-16 could modulate the angiogenesis of MM through regulating the VEGF expression. Furthermore, our data suggest that restoration of miR-15a and miR-16 may have considerable therapeutic potential in MM treatment.

Supplementary material

Supplementary Figures 1 and 2 can be found at http://carcin.oxfordjournals.org/

Funding

National Natural Sciences Foundation of China (No. 30700331 to C.Y.S.); National Natural Science Funds for Distinguished Young Scholar (No. 30825018 to Y.H.)

Conflict of Interest Statement: None declared.

References

1. Garzon,R. *et al.* (2006) MicroRNA expression and function in cancer. *Trends Mol. Med.*, **12**, 580–587.
2. He,L. *et al.* (2004) MicroRNAs: small RNAs with a big role in gene regulation. *Nat. Rev. Genet.*, **5**, 522–531.
3. Bartel,D.P. (2004) MicroRNAs: genomics, biogenesis, mechanism, and function. *Cell*, **116**, 281–297.
4. Mello,C.C. *et al.* (2004) Micromanaging insulin secretion. *Nat. Med.*, **10**, 1297–1298.
5. Baralle,M. *et al.* (2007) Genetics and molecular biology: micro RNAs are welcome to the lipid field. *Curr. Opin. Lipidol.*, **18**, 375–377.
6. Triboulet,R. *et al.* (2007) Suppression of microRNA-silencing pathway by HIV-1 during virus replication. *Science*, **315**, 1579–1582.
7. Calin,G.A. *et al.* (2006) MicroRNA-cancer connection: the beginning of a new tale. *Cancer Res.*, **66**, 7390–7394.
8. Calin,G.A. *et al.* (2006) MicroRNA signatures in human cancers. *Nat. Rev. Cancer*, **6**, 857–866.
9. Lu,J. *et al.* (2005) MicroRNA expression profiles classify human cancers. *Nature*, **435**, 834–838.
10. Blenkiron,C. *et al.* (2007) MicroRNA expression profiling of human breast cancer identifies new markers of tumor subtype. *Genome Biol.*, **8**, R214.
11. Dews,M. *et al.* (2006) Augmentation of tumor angiogenesis by a Myc-activated microRNA cluster. *Nat. Genet.*, **38**, 1060–1065.
12. Lee,D.Y. *et al.* (2007) MicroRNA-378 promotes cell survival, tumor growth, and angiogenesis by targeting SuFu and Fus-1 expression. *Proc. Natl. Acad. Sci. U.S.A.*, **104**, 20350–20355.
13. Barlogie,B. *et al.* (1997) Biology and therapy of multiple myeloma in 1996. *Semin. Hematol.*, **34**(1 Suppl 1), 67–72.
14. Munshi,N.C. *et al.* (2001) Increased bone marrow microvessel density in newly diagnosed multiple myeloma carries a poor prognosis. *Semin. Oncol.*, **28**, 565–569.
15. Vacca,A. *et al.* (2001) Bone marrow angiogenesis in patients with active multiple myeloma. *Semin. Oncol.*, **28**, 543–550.
16. Giuliani,N. *et al.* (2004) Angiogenic switch in multiple myeloma. *Hematology*, **9**, 377–381.
17. Ria,R. *et al.* (2003) Vascular endothelial growth factor and its receptors in multiple myeloma. *Leukemia*, **17**, 1961–1966.
18. Kumar,S. *et al.* (2003) Expression of VEGF and its receptors by myeloma cells. *Leukemia*, **17**, 2025–2031.
19. Dankbar,B. *et al.* (2000) Vascular endothelial growth factor and interleukin-6 in paracrine tumor-stromal cell interactions in multiple myeloma. *Blood*, **95**, 2630–2636.
20. Iwasaki,T. *et al.* (2002) Clinical significance of vascular endothelial growth factor and hepatocyte growth factor in multiple myeloma. *Br. J. Haematol.*, **116**, 796–802.
21. Di Raimondo,F. *et al.* (2000) Angiogenic factors in multiple myeloma: higher levels in bone marrow than in peripheral blood. *Haematologica*, **85**, 800–805.
22. Podar,K. *et al.* (2001) Vascular endothelial growth factor triggers signaling cascades mediating multiple myeloma cell growth and migration. *Blood*, **98**, 428–435.
23. Podar,K. *et al.* (2005) The pathophysiologic role of VEGF in hematologic malignancies: therapeutic implications. *Blood*, **105**, 1383–1395.
24. Hua,Z. *et al.* (2006) MiRNA-directed regulation of VEGF and other angiogenic factors under hypoxia. *PLoS ONE*, **1**, e116.
25. Roccaro,A.M. *et al.* (2009) MicroRNAs 15a and 16 regulate tumor proliferation in multiple myeloma. *Blood*, **113**, 6669–6680.
26. Sun,C.Y. *et al.* (2010) Brain-derived neurotrophic factor induces proliferation, migration, and VEGF secretion in human multiple myeloma cells via activation of MEK-ERK and PI3K/AKT signaling. *Tumour Biol.*, **31**, 121–128.
27. Sun,C. *et al.* (2009) The effect of brain-derived neurotrophic factor on angiogenesis. *J. Huazhong Univ. Sci. Technol. Med. Sci.*, **29**, 139–143.
28. Hu,Y. *et al.* (2007) Identification of brain-derived neurotrophic factor as a novel angiogenic protein in multiple myeloma. *Cancer Genet. Cytogenet.*, **178**, 1–10.
29. Calin,G.A. *et al.* (2008) MiR-15a and miR-16-1 cluster functions in human leukemia. *Proc. Natl. Acad. Sci. U.S.A.*, **105**, 5166–5171.
30. Cimmino,A. *et al.* (2005) miR-15 and miR-16 induce apoptosis by targeting BCL2. *Proc. Natl. Acad. Sci. U.S.A.*, **102**, 13944–13949.
31. Xu,J.L. *et al.* (2002) Proliferation, apoptosis, and intratumoral vascularity in multiple myeloma: correlation with the clinical stage and cytological grade. *J. Clin. Pathol.*, **55**, 530–534.
32. Lewis,B.P. *et al.* (2003) Prediction of mammalian microRNA targets. *Cell*, **115**, 787–798.
33. Betel,D. *et al.* (2008) The microRNA.org resource: targets and expression. *Nucleic Acids Res.*, **36**, D149–D153.
34. Nielsen,C.B. *et al.* (2007) Determinants of targeting by endogenous and exogenous microRNAs and siRNAs. *RNA*, **13**, 1894–1910.
35. Finnerty,J.R. *et al.* (2010) The miR-15/107 group of microRNA genes: evolutionary biology, cellular functions, and roles in human diseases. *J. Mol. Biol.*, **402**, 491–509.
36. Visone,R. *et al.* (2009) MiRNAs and cancer. *Am. J. Pathol.*, **174**, 1131–1138.
37. Esquela-Kerscher,A. *et al.* (2006) Oncomirs - microRNAs with a role in cancer. *Nat. Rev. Cancer*, **6**, 259–269.
38. Calin,G.A. *et al.* (2002) Frequent deletions and down-regulation of micro-RNA genes miR15 and miR16 at 13q14 in chronic lymphocytic leukemia. *Proc. Natl. Acad. Sci. U.S.A.*, **99**, 15524–15529.

39. Urbich,C. *et al.* (2008) Role of microRNAs in vascular diseases, inflammation, and angiogenesis. *Cardiovasc. Res.*, **79**, 581–588.
40. Fish,J.E. *et al.* (2009) MicroRNAs: opening a new vein in angiogenesis research. *Sci. Signal.*, **2**, pe1.
41. Wu,F. *et al.* (2009) Role of specific microRNAs for endothelial function and angiogenesis. *Biochem. Biophys. Res. Commun.*, **386**, 549–553.
42. Löffler,D. *et al.* (2007) Interleukin-6 dependent survival of multiple myeloma cells involves the Stat3-mediated induction of microRNA-21 through a highly conserved enhancer. *Blood*, **110**, 1330–1333.
43. Pichiorri,F. *et al.* (2008) MicroRNAs regulate critical genes associated with multiple myeloma pathogenesis. *Proc. Natl. Acad. Sci. U.S.A.*, **105**, 12885–12890.
44. Liu,B. *et al.* (2009) MiR-126 restoration down-regulate VEGF and inhibit the growth of lung cancer cell lines *in vitro* and *in vivo*. *Lung Cancer*, **66**, 169–175.
45. Mishra,P.J. *et al.* (2009) MicroRNA reexpression as differentiation therapy in cancer. *J. Clin. Invest.*, **119**, 2119–2123.
46. Trang,P. *et al.* (2011) Systemic delivery of tumor suppressor microRNA mimics using a neutral lipid emulsion inhibits lung tumors in mice. *Mol. Ther.*, **19**, 1116–1122.
47. Liu,C. *et al.* (2011) The microRNA miR-34a inhibits prostate cancer stem cells and metastasis by directly repressing CD44. *Nat. Med.*, **17**, 211–215.
48. Kota,J. *et al.* (2009) Therapeutic microRNA delivery suppresses tumorigenesis in a murine liver cancer model. *Cell*, **137**, 1005–1017.
49. Bonci,D. *et al.* (2008) The miR-15a-miR-16-1 cluster controls prostate cancer by targeting multiple oncogenic activities. *Nat. Med.*, **14**, 1271–1277.
50. Bandi,N. *et al.* (2009) miR-15a and miR-16 are implicated in cell cycle regulation in a Rb-dependent manner and are frequently deleted or down-regulated in non-small cell lung cancer. *Cancer Res.*, **69**, 5553–5559.
51. Wang,X. *et al.* (2008) Aberrant expression of oncogenic and tumor-suppressive microRNAs in cervical cancer is required for cancer cell growth. *PLoS ONE*, **3**, e2557.
52. Roldo,C. *et al.* (2006) MicroRNA expression abnormalities in pancreatic endocrine and acinar tumors are associated with distinctive pathologic features and clinical behavior. *J. Clin. Oncol.*, **24**, 4677–4684.
53. Liu,L. *et al.* (2010) microRNA-195 promotes apoptosis and suppresses tumorigenicity of human colorectal cancer cells. *Biochem. Biophys. Res. Commun.*, **400**, 236–240.
54. Wu,H. *et al.* (2009) Suppression of cell growth and invasion by miR-205 in breast cancer. *Cell Res.*, **19**, 439–448.
55. Corthals,S.L. *et al.* (2010) Micro-RNA-15a and micro-RNA-16 expression and chromosome 13 deletions in multiple myeloma. *Leuk. Res.*, **34**, 677–681.

Received May 2, 2012; revised October 7, 2012; accepted October 15, 2012